Dovepress

open access to scientific and medical research

Open Access Full Text Article

ORIGINAL RESEARCH

Yunnan Baiyao Might Mitigate Periodontitis Bone Destruction by Inhibiting Autophagy and Promoting Osteoblast Differentiation in vivo, ex vivo and in vitro

Wang Liu[1,2,*], Yanjie Li[1,2,*], Yuanyuan An[1,2], Ruoyu Zhao[1,2], Chenxi Wei[1,2], Xiaobin Ren[1], Hongbing He [1]

[1]Department of Periodontology, Kunming Medical University School and Hospital of Stomatology, Kunming, 650106, People's Republic of China; [2]Yunnan Key Laboratory of Stomatology, Kunming, 650106, People's Republic of China

*These authors contributed equally to this work

Correspondence: Hongbing He; Xiaobin Ren, Department of Periodontology, Kunming Medical University School and Hospital of Stomatology, Kunming, 650106, People's Republic of China, Tel +8613987196646; +8615877930860, Email hehongbing@kmmu.edu.cn; Renxiaobin6688@163.com

Background and Objective: Periodontitis is an inflammatory disease that eventually destroys tooth-supporting tissue. Yunnan Baiyao (YNBY), a traditional Chinese medicine compound with haemostatic and anti-inflammatory properties has shown therapeutic potential in several diseases. Our previous study revealed that YNBY suppressed osteoclast differentiation in periodontitis. The purpose of this study is to investigate the influences of YNBY on osteoblasts and explore its potential mechanisms.

Materials and Methods: A rat periodontitis model was established by ligation of maxillary second molars. After the end of modelling, histopathological observation by hematoxylin-eosin (HE) staining and Masson trichrome staining, detection of bone resorption by Micro-CT scanning, detection of osteoclasts by tartrate-resistant acid phosphatase (TRAP) staining, expression of osteocalcin (OCN) and microtubule-associated protein 1 light chain 3 (LC3) by immunohistochemistry. Lipopolysaccharides was used to irritate MC3T3-E1 osteoblastic cells and ex vivo calvarial organ as an in vitro model of inflammation. CCK-8 assay was performed to examine the toxicity of YNBY to MC3T3-E1 osteoblastic cells. Osteogenesis was assessed with alizarin red staining, immuno-fluorescence staining, Western blot and immunohistochemical staining. Transmission electron microscopy, fluorescent double staining, Western blot and immunohistochemical staining were employed to detect autophagy.

Results: Histological and micro-CT analyses revealed that YNBY gavage reduced bone loss caused by experimental periodontitis and upregulated osteogenic proteins in vivo. YNBY attenuated the production of autophagy-related proteins in periodontitis rats. Additionally, YNBY promoted osteogenesis by inhibiting inflammation-induced autophagy in vitro. Furthermore, YNBY suppressed LPS-mediated bone resorption and promoted the production of osteoblast-related proteins in inflamed calvarial tissues ex vivo.

Conclusion: This study demonstrated, through in vivo, in vitro and ex vivo experiments, that YNBY promoted osteoblast differentiation by suppressing autophagy, which markedly alleviated bone destruction caused by periodontitis.

Keywords: Yunnan Baiyao, periodontitis, osteoblasts, autophagy

Introduction

Periodontitis is a chronic oral disease caused by oral microbial flora dysbiosis and inflammation. Gingivitis, caused by plaque, is a reversible condition. If left untreated, it may progress to periodontitis, leading to attachment loss, bone destruction and ultimately tooth loss.[1,2] At present, restoring the structure and function of damaged tissue in periodontitis remains a significant clinical challenge.[3] An imbalance between bone homeostasis, ie, osteoclastic bone resorption is greater than osteoblastic bone formation, is the direct cause of alveolar bone loss.[4] During the development of periodontitis, plaque microorganisms and their toxins contribute to the destruction of periodontal tissue.[5] Lipopolysaccharides (LPS) from *Porphyromonas gingivalis* (Pg), a key periodontal bacterium, hinders osteoblast differentiation[6] and simultaneously promoting monocyte differentiation into osteoclasts.[7] Conversely, osteoclastogenesis inhibitory factor (osteoprotegerin, OPG), a soluble protein from osteoblasts,

2271

competes with receptor activator of nuclear factor-kappaB ligand (RANKL) to antagonize the RANK–RANKL interaction, thereby inhibiting osteoclastogenesis and preserving the osteogenic environment.[8,9] Therefore, osteogenesis is a key process in the inhibition of bone loss.

The expression of autophagy-related proteins increased in the gingival tissues of periodontitis patients.[10] Autophagy, which is involved in the metabolism of periodontal tissue[11] by regulating osteoblasts[12] and osteoclasts[13] in periodontitis, is activated during their differentiation. The deletion of autophagy-related gene 5 (Atg5) or autophagy-related gene 7 (Atg7) in mice resulted in reduced osteoblast numbers and autophagy in mice.[11,14,15] The adhesion and spreading of osteoclasts are affected by deficiency in the secretion function of lysosomes, which are involved in autophagy.[16] However, further exploration is needed to clarify how autophagy flux regulates bone metabolism in the inflammatory environment.

Yunnan Baiyao (YNBY), a traditional Chinese medicine compound, is primarily composed of the following types of traditional Chinese medicine: Tian Qi, San Yu Cao, Bai Niu Dan, Chuan Shan Long, Huai Shan Yao, Ku Liang Jiang, Lao Guan Cao, Bing Pian and Cao Wu.[17] The existence of YNBY serves as a testament to the profound ethnopharmacological legacy inherent in Eastern medicine. Previous studies have demonstrated the potential antibacterial,[18] antioxidant[17] and anti-inflammatory[19] properties of YNBY. Our earlier research also revealed that YNBY reduced the activity of overactive osteoclasts during periodontitis.[20] However, potential applications of YNBY for bone regeneration have not been explored, and the underlying mechanism by which YNBY regulates bone metabolism remains unaddressed. Significantly, the regulation of osteogenic remodelling through autophagy has been validated in traditional Chinese medicine.[21] Therefore, the potential mechanism by which YNBY modulates bone homeostasis may also be associated with autophagy.

In this research, we employed periodontitis animal, cell and ex vivo bone organ models, aiming to investigate the effects of YNBY on osteoblasts and bone metabolism and further explore its underlying mechanisms. The first null hypothesis of this study is that YNBY has no significant effect on osteoblasts and bone metabolism. The second null hypothesis of this study is that there is no significant change in autophagy flux under the intervention of YNBY.

Materials and Methods
LC-MS/MS Analysis
The UPLC-ESI-MS/MS system (UPLC, ExionLC™ AD; MS, Applied Biosystems 6500 Q TRAP) used Agilent SB-C18 column with a gradient program of solvent A (pure water with 0.1% formic acid) and solvent B (acetonitrile with 0.1% formic acid). The column temperature was maintained at 40°C, and the injection volume was 2 μL. The effluent was directed to an ESI-Q TRAP-MS/MS were set for effective analysis of the drug. The data were gathered and analyzed utilizing the LC-MS/MS-associated software (Table 1 and Table S1).

Table 1 The Nine Components of Yunnan Baiyao

No.	Q1 (Da)	Q3 (Da)	Molecular Weight (Da)	Formula	Ionization Model	Compounds
1	1107.5900	1107.5900	1108.6029	C54H92O23	[M-H]-	Notoginsenoside Rb1
2	829.5000	769.4800	830.5028	C43H74O15	[M-H]-	Ginsenoside ST-3
3	841.5000	781.4800	842.5028	C44H74O15	[M-H]-	Vina-Ginsenoside R1
4	1123.5900	1123.5900	1124.5979	C54H92O24	[M-H]-	Notoginsenoside A
5	811.4900	751.4700	812.4922	C43H72O14	[M-H]-	Sanchirhinoside A2
6	753.4800	423.3600	752.4711	C41H68O12	[M+H]+	Notoginsenoside T5
7	637.4300	421.3500	636.4237	C36H60O9	[M+H]+	ginsenoside Rh5/7/8
8	933.5400	295.1000	932.5345	C47H80O18	[M+H]+	ginsenoside Re4
9	933.5400	295.1000	932.5345	C47H80O18	[M+H]+	Notoginsenoside R1

Notes: Q1 (Da): The molecular weight of the parent ion after ionization by electrospray ionization source; Q3 (Da): characteristic fragment ions.

Experimental Periodontitis Model (in vivo)

A total of 18 male Sprague Dawley (SD) rats, with a weight of 180 g and of SPF grade, were used for the experiment. All rats were in good health, with no oral or systemic diseases, and no missing teeth. All rats were housed in a controlled environment (25°C, 50% humidity, and a 12 h light–dark cycle) with free access to water and food. YNBY (China Yunnan Baiyao Group Co., Ltd., Kunming, China) was dissolved in 0.5% sodium carboxymethyl cellulose (CMC-Na) as a vehicle. The rats were randomly divided into the following groups, each consisting of six rats: (1) control group (Control) (without ligature or oral YNBY administration); (2) periodontitis group (Periodontitis) (with ligature and oral CMC-Na administration); and (3) periodontitis + YNBY group (P + YNBY) (with ligature and oral YNBY administration). Experimental periodontitis was induced in rats by ligating the maxillary second molar teeth using a needle holder to place ligature thread, and 4 weeks later, YNBY was orally administered at a dose of 50 mg per animal daily (Figure 1). After 6 weeks, all rats were euthanized by cervical dislocation, and maxillary samples were collected using scissors.

Microcomputed Tomography (Micro-CT) Scanning

The maxillary samples were fixed in 4% paraformaldehyde for 24 h and scanned using a NEMO NMC-100 micro-CT system (PINGSENG Healthcare Inc., Kunshan, China). Each maxilla was scanned separately at a 90 kV source voltage, 60 μA source current and 7.5 μm resolution. Mimics Research software (version 17.0; Materialise NV, Leuven, Belgium) was employed to reconstruct three-dimensional images and measure the distance between the cemento-enamel junction and the alveolar bone on both the buccal and palatal surfaces of the second molar to assess bone loss.

Histological Analysis

The samples were decalcified with EDTA solutions (pH 7.2, X2776, Leagene Biotechnology, Beijing, China) for 4 weeks at room temperature, changing twice a week. Dehydration was performed with gradient alcohol, followed by paraffin embedding. Sections of 4 μm were prepared using a conventional method. Hematoxylin-eosin (HE) staining, Masson trichrome staining (G1006, Servicebio, Hubei, China) and tartrate-resistant acid phosphatase (TRAP) staining (G1492, Solarbio, Beijing, China) were carried out following the manufacturer's instructions.
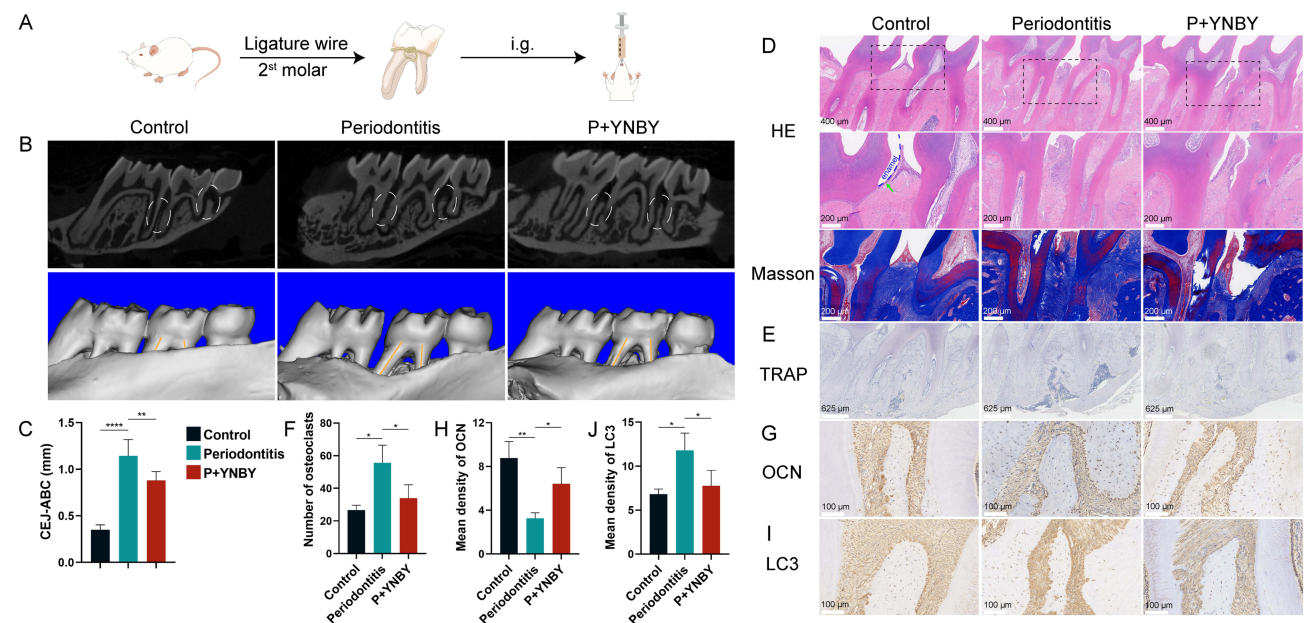

Figure 1 YNBY reduces alveolar bone loss in periodontitis rats. (**A**) Modelling steps of the periodontitis rat model. (**B**) Three-dimensional and two-dimensional micro-CT reconstruction of rat alveolar bone; dotted circle lines, interdental alveolar crestal bone; solid lines, direction of tooth root. (**C**) Quantitative analysis of distance from the CEJ to ABC. (**D**) Histological staining of alveolar bones, including H&E and Masson trichrome staining; green arrows, enamel; low-magnification scale bar, 400 μm; high-magnification scale bar, 200 μm. (**E** and **F**) TRAP staining of alveolar bones (**E**) and quantitative analysis of osteoclast number (**F**); scale bar, 625 μm. (**G**) Immunohistochemistry of OCN; scale bar, 100 μm. (**H**) Quantitative analysis of the immunohistochemistry in G. (**I**) Immunohistochemistry of LC3; scale bar, 100 μm. (**J**) Quantitative analysis of the immunohistochemistry in I. Data are expressed as the mean ± SD; *p < 0.05; **p < 0.01; ****p < 0.0001.

Immunohistochemical (IHC) staining was performed to assess the expression levels of osteocalcin (OCN) (GB11233-100, Servicebio, Hubei, China, 1:100), osteoprotegerin (OPG) (bs-20624R, Bioss, Beijing, China, 1:200), microtubule-associated protein 1 light chain 3 (LC3) (14600-1-AP, Proteintech, Hubei, China, 1:200) and autophagy-related protein 5 (ATG5) (10181-2-AP, Proteintech, Hubei, China, 1:200). After conventional dewaxing and hydration, antigen repair was conducted with EDTA solution (MVS-0099, Maixin, Biotech) (OCN, OPG) or citrate buffer (MVS-0101, Maixin Biotech) (LC3, ATG5) at 100°C for 30 min. After natural cooling to room temperature, the slides were rinsed in phosphate buffered saline (PBS) for 5 min, and an endogenous peroxidase blocker (SP KIT-A3, Maixin Biotech) was used to block endogenous peroxidase activity for 15 min. Following three 5-min rinses with PBS, the slides were incubated with the anti-OCN antibody, anti-OPG antibody, anti-LC3 antibody and anti-ATG5 antibody at 4°C overnight. The next day, the slides were washed thrice in PBS and incubated with the secondary biotinylated antibody from the MaxVision HRP-Polymer anti-Mouse/Rabbit IHC Kit (KIT-5020, Maixin Biotech) at room temperature for 1 hour. After the slides were washed thrice in PBS, the immunohistochemical reactions were visualized with a DAB chromogen kit (DAB-0031, Maixin Biotech), and haematoxylin was used for nuclear staining in all tissue sections. Finally, the slides were dehydrated by gradient dehydration with ethanol, permeated in xylene and mounted with resin. Deep brown staining was considered an immunopositive reaction.

The stained sections were scanned using a KF-PRO-005 digital slide scanner (KFBIO, Ningbo, China) and analysed with K-Viewer software (KFBIO, version 1.7.0.27). Quantitative analysis of the optical density was conducted by Image-Pro Plus v6.0 (Media Cybernetics).

Ex vivo Calvarial Organ Cultures

Calvarial organs were obtained from newborn C57 sucking mice at 3 days of age. The calvariae were removed by cutting around the cranial sutures (Figure 2H, lines 1, 2, 3) and washed in PBS containing 10% penicillin-streptomycin (HyClone, USA). Each calvaria was maintained in 24-well plates with Dulbecco's modified Eagle's medium (DMEM) (C11995500BT, Gibco) containing 10% foetal bovine serum (C04001-050X10, VivaCell, Shanghai, China) and 1% penicillin streptomycin. Tissues were stained using the same procedure as described above after LPS and YNBY intervention.

Cell Line

The mouse preosteoblast cell line MC3T3-E1 Subclone 14 (GNM15) was kindly provided by Cell Bank, Chinese Academy of Sciences and maintained in α-MEM medium (C12571500BT, Gibco) supplemented with 10% foetal bovine serum. Cells were cultured at 37°C in a humidified atmosphere containing 5% CO_2.

CCK-8 Assay

Dimethyl sulfoxide (DMSO) (D8371, Solarbio, Beijing, China) was used as a medium to dissolve YNBY (DMSO < 0.01% in all experiments). Cells were seeded in 96-well plates and treated with various concentrations of YNBY (0, 5, 10, 20 and 40 μg/mL) and DMSO. At 0, 1, 3, 5, and 7 days, the cells were incubated with 10 μL CCK8 solution (Dojindo, Kumamoto, Japan) to assay the cytotoxic effect of YNBY. After 2 h at 37°C, the absorbance at 450 nm was measured for each well, and cell viability curves were plotted. The experiments were repeated three times.

In vitro Osteoblast Differentiation

Cells were plated on 6-well plates containing α-MEM supplemented with 10% foetal bovine serum, 50 μM L-ascorbic acid (D4544, Sigma), 10 mM β-glycerolphosphate (D9422, Sigma), and 10 nM dexamethasone (D4902, Sigma). To investigate the effect of YNBY on the osteogenic differentiation of MC3T3-E1 cells in inflammatory environments, the cells were randomly divided into the following groups: (1) osteogenesis-inducing culture medium group (Control); (2) osteogenesis-inducing culture medium group containing DMSO group (DMSO); (3) osteogenesis-inducing culture medium group containing DMSO and 10 μg/mL LPS (L2880, Sigma) group (LPS); and (4) osteogenesis-inducing culture medium group containing DMSO, 10 μg/mL LPS and 20 μg/mL YNBY group (LPS + YNBY). After 4 weeks of
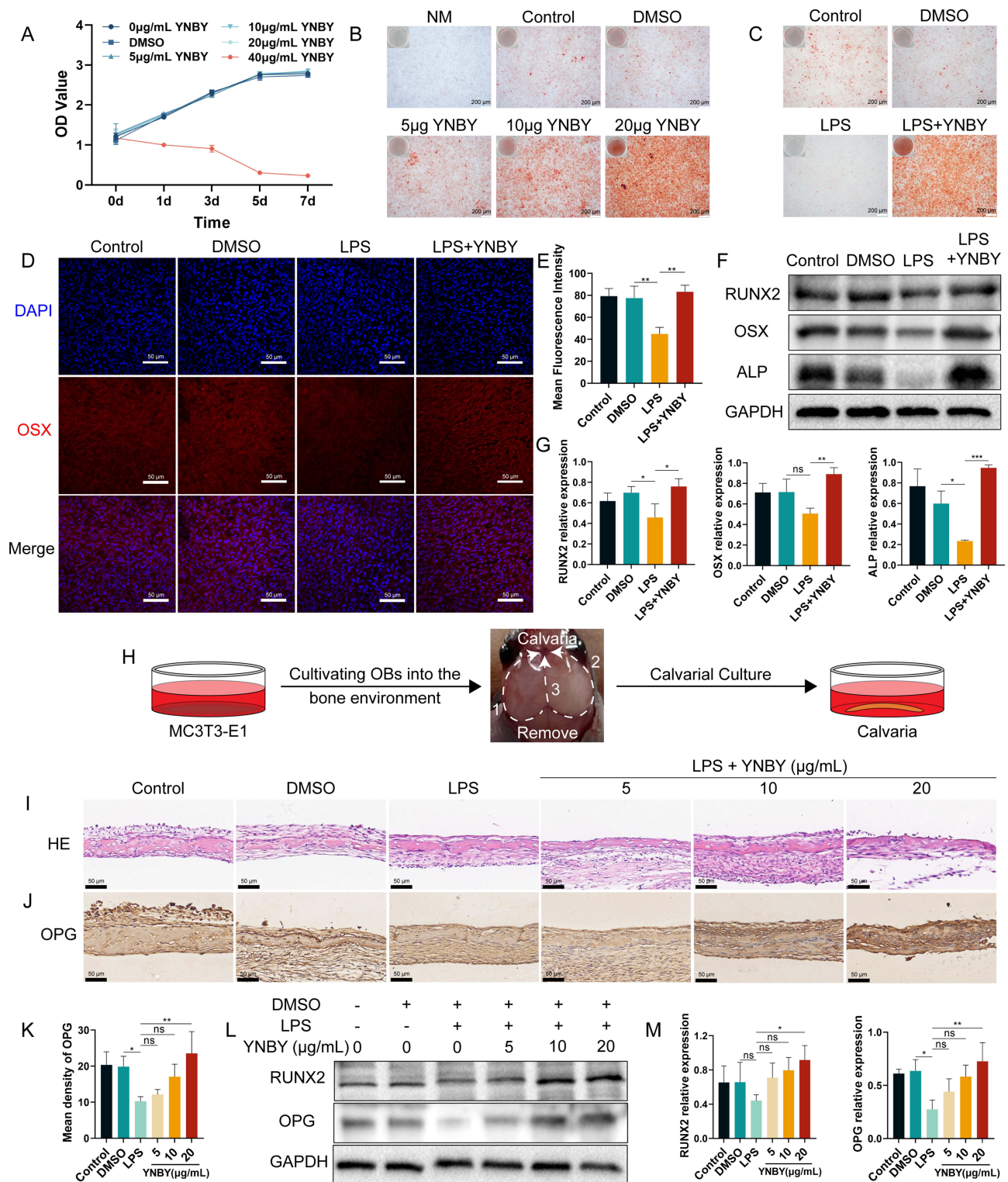
Figure 2 YNBY promotes osteogenic differentiation in an inflammatory environment. (**A**) CCK-8 assay of MC3T3-E1 cells after treatment with YNBY (0, 5, 10, 20 and 40 μg/mL) or DMSO for 0, 1, 3, 5 and 7 days. (**B**) Alizarin Red staining of MC3T3-E1 cells treated with different concentrations of YNBY; scale bar, 200 μm. (**C**) Alizarin Red staining of MC3T3-E1 cells treated with 20 μg/mL YNBY under LPS-induced inflammation; scale bar, 200 μm. (**D** and **E**) Immunofluorescence staining (**D**) and quantitative analysis (**E**) of OSX in MC3T3-E1 cells; scale bar, 50 μm. (**F** and **G**) Western blot (**F**) and quantificational analysis (**G**) of RUNX2, OSX and ALP in MC3T3-E1 cells. (**H**) Schematic diagram of the steps of calvarial anatomy. (**I**) Representative H&E staining of calvaria; scale bar, 50 μm. (**J** and **K**) Immunohistochemical staining (**J**) and quantitative analysis (**K**) of OPG in calvaria; scale bar, 50 μm. (**L** and **M**) Western blot (**L**) and quantification (**M**) of RUNX2 and OPG in calvaria treated with LPS and different concentrations of YNBY. Data are expressed as the mean ± SD; n = 3; *p < 0.05; **p < 0.01; ***p < 0.001, ns = not significant.

induction, the mineralized nodules of osteoblast differentiation were observed through the application of Alizarin Red S Solution (ALIR-10001, OriCell, Guangzhou, China).

Western Blotting

After 7 days of osteogenic induction in a 6-well plate, total proteins were extracted from the cells by RIPA Buffer (R0010, Solarbio, Beijing, China) including protease inhibitor mixture. The calvarias were ground into powder in adequate liquid nitrogen, and then RIPA buffer (10 μL/mg) including a protease inhibitor mixture was added. Equal amounts of the protein samples were separated by electrophoresis on proper SDS-PAGE polyacrylamide gels (10%, 15%). Then the samples were transferred to PVDF membranes (0.22 μm, Millipore) using a wet transfer apparatus (Bio-Rad) and blocked with blocking buffer (P0252, Beyotime, Shanghai, China) for 30 min at room temperature. The membranes were incubated with primary antibodies at 4°C overnight. Afterwards, the blots were incubated with secondary antibodies (SA00001-2, Proteintech, Hubei, China, 1:5000) at room temperature for 1 h. The Super-sensitive ECL chemiluminescent substrate (BL520A, Biosharp, Anhui, China) was used to detect the protein bands. Band intensities were relatively quantified using ImageJ software (1.35q; Wayne Rasband, NIH). The primary antibodies used were as follows: Glyceraldehyde-3-phosphate dehydrogenase (GAPDH) (#380646, zenbio, Chengdu, China, 1:7500), Runt-related transcription factor 2 (RUNX2) (#bs-1134R, Bioss, 1:1000), Osterix (OSX) (#bs-1110R, Bioss, 1:1000), alkaline phosphatase (ALP) (#ab229126, abcam, 1:1000), osteoprotegerin (OPG) (#bs-20624R, Bioss, 1:1000), Receptor Activator for Nuclear Factor-κ B Ligand (RANKL) (#bs-0747R, Bioss, 1:1000), Recombinant Nuclear Factor Of Activated T Cells, Cytoplasmic 1 (NFATC1) (#66963-1-Ig, Proteintech, 1:6000), Recombinant Matrix Metalloproteinase 9 (MMP9) (#bs-41146R, Bioss, 1:1000), Recombinant Cathepsin K (CTSK) (bs-1611R, Bioss, 1:1000), Sequestosome 1 (P62/SQSTM1) (#18420-1-AP, Proteintech, 1:25000), microtubule-associated proteins light chain 3 (LC3) and (#14600-1-AP, Proteintech, 1:3000).

Immunofluorescence Staining

The cells were seeded in a confocal dish. After 7 days, the cells were fixed in 4% paraformaldehyde for 30 min and permeabilized with 0.1% Triton X-100 in PBS for 20 min. Then, the cells were blocked with 5% BSA for 30 min in PBS followed by incubation with anti-OSX antibody (1:200) at 4°C overnight. Afterwards, the cells were incubated with fluorescent secondary antibodies (a23420, abbkine, Georgia, USA, 1:200) at 37°C for 1 h. Nuclei were stained with DAPI solution (C0065, Solarbio) for 5 min at room temperature. Finally, fluorescence staining was visualized using a laser scanning confocal microscope (Nikon, Tokyo, Japan).

Autophagy Flux Detection

The cells were seeded in a confocal dish. According to the manufacturer's instructions, the cells were infected with adenovirus expressing mRFP-GFP-LC3 (Hanbio, Shanghai, China) to assess autophagic flux. In brief, 100 MOI virus solution was added to each confocal dish after seeding in the confocal dish overnight. After a 4 h incubation, an equal volume of fresh culture medium was added to the confocal dish. After a 10 h incubation, the culture medium containing the virus was replaced with fresh osteogenesis-inducing culture medium. After another 6 h of incubation, the cells were washed three times with PBS and fixed with 4% paraformaldehyde solution for 15 min. Autophagosomes and autolyso-somes were observed by a laser scanning confocal microscope.

Transmission Electron Microscopy (TEM)

The number and morphology of autophagosomes and autolysosomes were observed by a transmission electron microscope (JEM-1400FLASH, Japan). Briefly, the cells in each group were digested and centrifuged. The cell pellets were fixed with 3% glutaraldehyde and then fixed with 1% osmium tetroxide. After fixation, the cell pellets were dehydrated by gradient acetone. Then, the samples were embedded in Epon812 epoxy resin to prepare ultrathin sections (60–90 nm). After being stained with uranyl acetate and lead citrate, the autophagosomes and autolysosomes were observed by TEM.

Statistical Analysis

Data are expressed as the mean ± SD, and P values less than 0.05 were considered statistically significant. The number of samples or images analysed is indicated in each figure legend. Comparisons between multiple groups were performed using one-way ANOVA, and normality tests were performed before performing statistical analysis. All statistical tests were performed using GraphPad Prism 9.0. Software (USA).

Results

YNBY Reduces Alveolar Bone Loss in Periodontitis Rats

Periodontitis-induced alveolar bone loss was quantified by linearly measuring the distance from the cement-enamel junction to the alveolar bone crest (CEJ-ABC) of the maxillary second molar. Micro CT showed that the significant increase in the CEJ-ABC distance of Periodontitis group showed considerable alveolar bone resorption, illustrating the success construct of the rat periodontitis disease model, and alveolar bone resorption was lessened after YNBY intervention (Figure 1A–C). Histological staining was used to detect pathological damage to the periodontal tissue, H&E staining indicated inflammatory infiltration, and Masson trichrome staining indicated collagen fibre rearrangement. The results showed that marked inflammatory infiltration, blood vessel congestion, and the arrangement of fibroblasts and collagen fibres were visibly disordered and that the junctional epithelium migrated towards the root in the Periodontitis group compared with the Control group, which was reversed by YNBY (Figure 1D). YNBY significantly downregulates osteoclast numbers in rat periodontitis models (Figure 1E and F), which results in a reduction in alveolar bone resorption. IHC analysis of OCN expression in osteoblasts in the Periodontitis group was reduced relative to that in the Control group. After YNBY gavage intervention, OCN expression increased (Figure 1G and H), indicating that YNBY intervention promoted osteoblast differentiation in periodontal tissue. These results were consistent with the micro-CT results. Simultaneously, YNBY reduces the expression of LC3 in periodontal tissue caused by periodontitis (Figure 1I and J). These observations suggest that YNBY significantly inhibits bone resorption and promotes osteogenesis.

YNBY Promotes Osteogenic Differentiation in an Inflammatory Environment

The CCK8 assay was used to assess the toxicity of YNBY to MC3T3-E1 cells. A concentration of YNBY greater than or equal to 40 μg/mL exhibited significant toxicity on cell viability (Figure 2A). Therefore, YNBY was used at concentrations lower than or equal to 20 μg/mL for the subsequent experiments to avoid cytotoxicity. Alizarin red staining revealed that YNBY intervention promoted osteogenesis in a dose-dependent manner and alleviated osteogenic inhibition caused by exposure to 10 μg/mL LPS at the same time (Figure 2B and C). Consistently, the Western blotting results showed that the YNBY-treated groups showed increased expression of osteogenesis-related proteins (RUNX2, OSX and ALP) compared with the LPS group (Figure 2F and G), and the upregulation of OSX expression was further confirmed by immunofluorescence (Figure 2D and E).

To further confirm the effect of YNBY on osteogenesis, we used ex vivo calvarial organ cultures, which expose osteoblasts to the bone environment (Figure 2H). We established a model for LPS-induced bone resorption in ex vivo calvaria to mimic bone resorption initiated by inflammation. HE staining showed that LPS increased infiltration of inflammatory cells (Figure S1A). TRAP staining showed that as the concentration of LPS increased, the number of osteoclasts increased (Figure S1B and C). Western blot results showed that the expression of osteoclast-specific proteins (NFATC1, MMP9 and CTSK) was upregulated by LPS (Figure S1D and E), suggesting that LPS can successfully cause bone resorption. LPS-induced bone resorption was suppressed by different concentrations of YNBY (Figure S1F and G). Simultaneously, immunohistochemical results revealed that the OPG protein level was increased in the calvaria of the YNBY group relative to the LPS group (Figure 2I–K). The results of Western blot analysis also showed that YNBY intervention decreased the expression levels of osteoclast-related marker proteins (NFATC1, MMP9 and RANKL) (Figure S1H and I) and increased the expression levels of osteogenesis-related marker proteins (RUNX2 and OPG) (Figure 2L and M). These results suggest that YNBY can inhibit bone resorption and promote osteogenic differentiation.

YNBY Inhibits Autophagy in the Inflammatory Environment

GFP-RFP tandem fluorescent-tagged LC3 observed by a laser scanning confocal microscope showed that yellow and red spots were increased in the LPS group, suggesting that LPS can activate autophagy flux by enhancing autophagosome conversion to autolysosomes;[22] however, this process was inhibited by YNBY (Figure 3A and B). As GFP green fluorescent protein is sensitive to acidity, GFP green fluorescence is quenched after acidic lysosomes fuse with autophagosomes to form autolysosomes, and only RFP red fluorescence can be detected.[23] Furthermore, transmission electron microscopes revealed that the numbers of double-membrane autophagosomes and single-membrane autolysosomes were dramatically reduced in the LPS+YNBY group compared with those in the LPS group (Figure 3C). Consistent with this finding, Western blot analysis revealed decreases in the ratio of LC3 II/LC3 I and increases in P62 levels in the YNBY-treated group (Figure 3D and E), indicating the obstruction of autophagy.

Immunohistochemical analysis showed that the expression of ATG5 in calvarial bone tissue increased with LPS and was inhibited by YNBY (Figure 3F and G). The Western blot results were also consistent with the cell experiments (Figure 3H and I). This evidence indicates that YNBY reversed the increased autophagic flux caused by LPS treatment.

YNBY Promotes Osteogenic Differentiation Through Inhibiting Inflammation-Induced Autophagy

To test whether autophagy flux is involved in YNBY-induced osteoblast differentiation, we added the autophagy agonist RAPA and inhibitor 3-MA to treat cells under LPS and YNBY cotreatment. Double fluorescent tagged LC3 and visualized autophagosome structure under the transmission electron microscope showed that RAPA promoted the combination of autophagosomes and lysosomes, but 3-MA generated the opposite effect (Figure 4A–C). Western blot results of LC3 and P62 further demonstrated the same results (Figure 4D and E). The above observations indicate that the autophagy agonist RAPA completely abolished the YNBY-mediated inhibition of autophagy, but the inhibitor 3-MA further promoted the
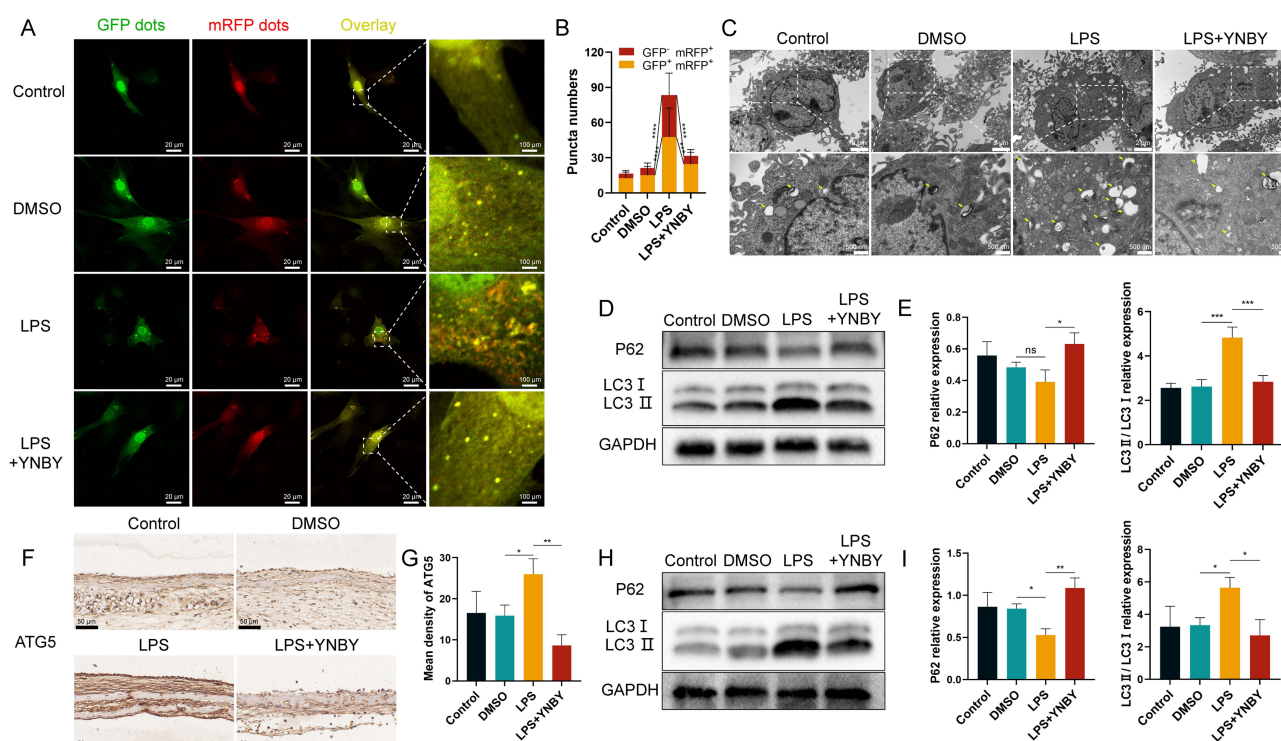

Figure 3 YNBY inhibits autophagy in an inflammatory environment. (**A** and **B**) Autophagic flux detection for MC3T3-E1 cells transfected with adenovirus expressing mRFP-GFP-LC3 (**A**) and quantitative analysis (**B**); scale bar, 20 μm; n=30. (**C**) Transmission electron microscopy of MC3T3-E1 cells; low-magnification scale bar, 2 μm; high-magnification scale bar, 500 nm. (**D** and **E**) Western blot (**D**) and quantificational analysis (**E**) of autophagy in MC3T3-E1 cells; n=3. (**F** and **G**) Immunohistochemical staining (**F**) and quantitative analysis (**G**) of ATG5 in calvaria; scale bar, 50 μm; n=3. (**H** and **I**) Western blot (**H**) and quantificational analysis (**I**) of autophagy in calvaria; n=3. Data are expressed as the mean ± SD; n = 3; *p < 0.05; **p < 0.01; ***p < 0.001; ****p < 0.0001, ns = not significant.
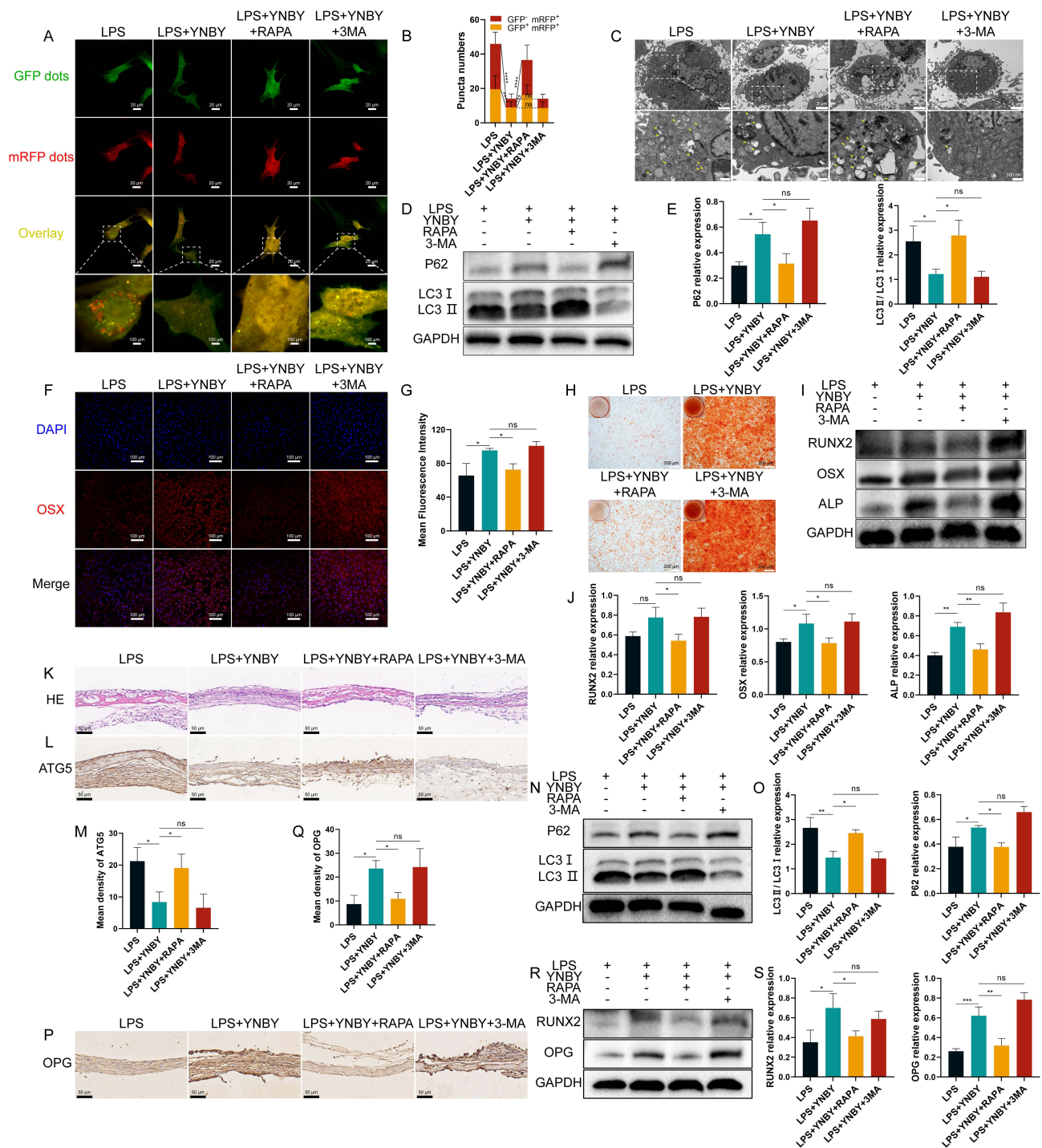
Figure 4 YNBY promotes osteogenic differentiation by inhibiting inflammation-induced autophagy. (**A** and **B**) Autophagic flux detection for MC3T3-E1 cells transfected with adenovirus expressing mRFP-GFP-LC3 (**A**) and quantitative analysis (**B**); scale bar, 20 μm; n=30. (**C**) Transmission electron microscopy of MC3T3-E1 cells; low-magnification scale bar, 2 μm; high-magnification scale bar, 500 nm. (**D** and **E**) Western blot (**D**) and quantification (**E**) of autophagy in MC3T3-E1 cells; n=3. (**F** and **G**) Immunofluorescence staining (**F**) and quantitative analysis (**G**) of OSX in MC3T3-E1 cells; scale bar, 50 μm; n=3. (**H**) Alizarin Red staining of MC3T3-E1 cells; scale bar, 200 μm; n=3. (**I** and **J**) Western blot (**I**) and quantification (**J**) of RUNX2, OSX and ALP in MC3T3-E1 cells; n=3. (**K** and **L**) Representative H&E staining (**K**) and immunohistochemical staining of ATG5 (**L**) in calvaria; scale bar, 50 μm. (**M**) Quantitative analysis of the immunohistochemistry in L, n=3. (**N** and **O**) Western blot (**N**) and quantificational analysis (**O**) of autophagy in calvaria; n=3. (**P** and **Q**) Immunohistochemical staining (**P**) and quantitative analysis (**Q**) of OPG in calvaria; scale bar, 50 μm; n=3. (**R** and **S**) Western blot (**R**) and quantificational analysis (**S**) of RUNX2 and OPG in calvaria; n=3. Data are expressed as the mean ± SD; *p < 0.05; **p < 0.01; ***p < 0.001; ****p < 0.0001, ns = not significant.
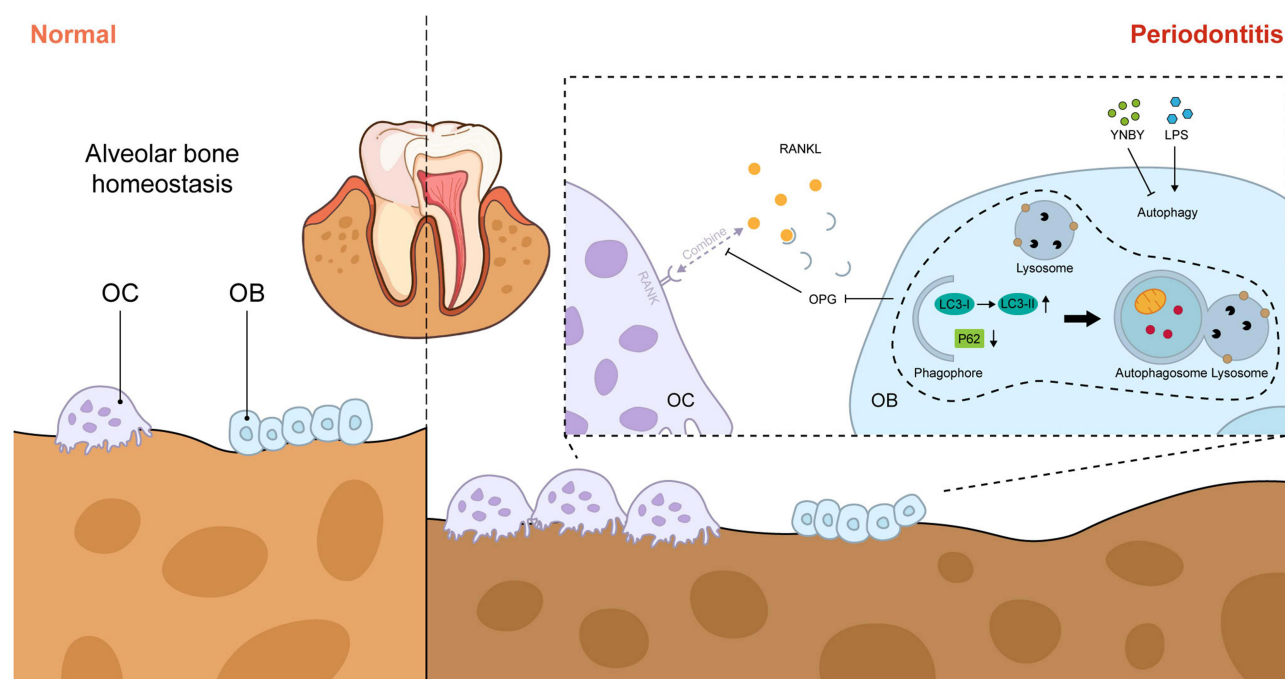
Figure 5 Pattern diagram for the mitigation of periodontitis-induced bone destruction by YNBY, which promotes osteoblast differentiation through inhibiting autophagy. The figure was created using Adobe Illustrator.

inhibition of autophagy by YNBY. Notably, incubation with the autophagy agonist RAPA significantly reversed the promotion of osteogenic differentiation by YNBY in inflammatory environment, with fewer calcium deposits (Figure 4H) and lower expression of osteogenesis-related proteins (Figure 4F–J). Application of the autophagy inhibitor 3-MA reached the icing on the cake effect on the promotion of osteogenic differentiation (Figure 4F–J). The involvement of autophagy in osteogenic differentiation induced by YNBY was validated by RAPA and 3-MA.

Although YNBY could inhibit osteoclast differentiation and promote osteogenic differentiation in calvarial inflammatory environments, RAPA inhibited the effects of YNBY while upregulating autophagy flux (Figure 4K–S and Figure S2A–D). Moreover, 3-MA generated the opposite effect (Figure 4K–S and Figure S2A–D). Conclusively, YNBY attenuated bone loss by inhibiting the formation, differentiation, and bone resorption activities of osteoclasts and promoting bone formation and osteogenic differentiation by inhibiting inflammation-induced autophagy (Figure 5).

Discussion

This study was designed to identify whether YNBY promoted osteoblast differentiation while inhibiting bone resorption in periodontitis and to explore the underlying mechanisms. Our experiments showed that oral YNBY administration reduced alveolar bone resorption in a rat periodontitis model and improved osteogenic activity. LPS was used to mimic inflammation in vitro to inhibit osteogenic differentiation. Then, the effects of YNBY on MC3T3-E1 osteogenic differentiation in the inflammatory microenvironment and the underlying mechanisms were investigated. The results showed that YNBY reversed LPS-induced osteogenic inhibition. The involvement of autophagy flux in YNBY-mediated osteogenic differentiation was confirmed through rescue experiments with the autophagy agonist RAPA and inhibitor 3-MA. Finally, YNBY-treated ex vivo calvarial organ culture models were established to mimic the natural remodelling state of bones in vivo, and the same results were observed.

Periodontitis initially involves the accumulation of many periodontal pathogenic bacteria, leading to ecological imbalance in the oral microbiota; as a result, inflammation occurs and the integrity of tooth-supporting tissues is decreased.[24] YNBY has shown significant potential for periodontitis treatment inhibiting periodontitis progression by reducing osteoclast differentiation,[19,20] but its role in osteoblast differentiation remains unspecified. This study revealed that YNBY upregulated osteogenesis-related protein expression (OCN) while inhibiting osteoclast differentiation based on previous research.[20] In

addition, the junctional epithelium migrates apically resulting in the formation of a deep periodontal pocket as periodontitis advances.[25] YNBY improved the attachment site of the newly formed junctional epithelium and the renewal of the underlying connective tissue. In addition, the shape of the dental papilla was partially restored, indicating that YNBY exhibits positive effects on alveolar bone regeneration and soft tissue healing. However, the specific mechanism by which YNBY regulates osteoblasts remains to be further explored. It has been reported that elevated levels of autophagy gene expression are observed in peripheral blood of patients with periodontitis.[26] Metabolites of periodontal pathogenic bacteria, such as Hydrogen sulfide (H2S), exacerbate alveolar bone loss in periodontitis rats, while upregulating the expression levels of autophagy-related proteins LC3 and Beclin-1.[27] Dang et al found that inhibiting autophagy can restore the osteogenic differentiation potential of stem cells and improve alveolar ridge preservation.[28] In our study, we found that YNBY not only promotes bone regeneration but also reduces the expression of autophagy protein LC3 elevated due to periodontitis, suggesting that autophagy may play a regulatory role in the bone repair process of YNBY.

In periodontitis, enhanced alveolar bone loss was determined by an imbalance between osteoblasts and osteoclasts,[29] manifesting as continuous activation of osteoclasts[30] and delayed bone formation by osteoblasts. Historically, research on periodontitis has been confined to the regulation of individual osteoblast cells.[31,32] Therefore, in addition to investigating the effects of YNBY on osteoblasts using a cell model, we utilized an ex vivo calvarial organ model to explore the impact on bone regeneration within the natural extracellular matrix environment in the presence of osteoclasts. Cultured bone explants preserve the in vivo 3D distribution of osteocytes and thus maintain the natural position within the extracellular mineralized matrix; as a result, these explants are often used as an in vitro model to investigate the effects of drugs on bone metabolism.[33] Compared to in vivo animal models, the ex vivo bone organ culture system is less expensive, faster, and eliminates interference by hormones, mechanical stimulation, and other factors present in animals. Ex vivo bone organ cultures combine the advantages of animal models and cell cultures, providing a unique research option.[34] Alveolar bone is formed through intramembranous ossification,[35] and its histologic appearance, structure and biological characteristics are similar to those of calvaria. The ex vivo calvarial organ culture system is an appropriate method for assessing the resorption of alveolar bone.

The RANKL/RANK/OPG pathway is an essential signalling pathway related to bone metabolism that plays an important role in osteogenesis and bone remodelling.[36] OPG, a soluble decoy receptor, neutralizes RANKL, preventing it from binding to RANK, which is the only functional receptor for RANKL; as a result, an osteoprotective effect is achieved.[37] Our research aligns with findings by Kadriu et al,[38] demonstrating that YNBY positively regulates osteoblast expression of OPG while repressing RANKL, thereby decreasing osteoclastogenesis. Cooperative activity regulation between bone-resorbing osteo-clasts and bone-building osteoblasts is needed to maintain normal bone metabolism.[39] Therefore, the main function of YNBY is to restore imbalanced bone homeostasis due to prolonged inflammatory infiltration.

As a self-phagocytosis and self-protection mechanism, autophagy is associated with osteoblast differentiation and mineralization.[11] According to Li et al, AMPK activation stimulates osteoblast differentiation and mineralization through autophagy.[40] NOLLET et al found that knockout of autophagy-related genes (BECN-1, ATG7, LC3) reduces the mineraliza-tion ability of osteoblasts, leading to insufficient bone formation.[11] Recent studies have shown that autophagy can promote osteoblast differentiation by increasing the Wnt/β-catenin signaling pathway.[12] Activation of autophagic flux can promote osteoblast differentiation, secretion of bone matrix, thus regulating bone remodeling,[21] but excessive or prolonged autophagic activity can lead to bone loss and decreased bone strength.[41] Reactive oxygen species (ROS) are after-products of cellular metabolism, including free radicals, peroxides, and oxygen ions, and they are closely associated with inflammation[42] and cellular damage.[43] As periodontitis progresses, excessive ROS can disturb autophagy, trigger an intensive inflammatory immune response, and destroy periodontal tissue.[44,45] Our results showed that the increased autophagy induced by LPS inhibited osteogenic differentiation, which may be caused by excessive autophagy. The potential mechanisms may involve cellular damage caused by excessive ROS, which prevents the osteogenic differentiation process. Similarly, Dang et al found that inhibiting inflammation-induced autophagy can restore the osteogenic differentiation potential of human dental pulp stem cells (hDPSCs).[28] The relationship between YNBY and autophagy has been reported in our published article, in which YNBY was found to inhibit osteoclast differentiation by blocking autophagy flux.[20] The results obtained in the current study complement our earlier research. Collectively, the work presented in this paper indicates that YNBY regulates bone home-ostasis by promoting osteoblast differentiation and inhibiting osteoclast development through the blockade of autophagy flux in the context of periodontal inflammation (Figure 5).

Admittedly, this study has several noteworthy limitations. Firstly, it remains unclear precisely how YNBY impacts autophagy or its upstream factors, necessitating in-depth study in further research. Secondly, the therapeutic efficacy of YNBY in treating bone loss in periodontitis requires further clinical validation before its clinical application.

Conclusion

In conclusion, this research indicates that YNBY can promote osteoblast differentiation and inhibit osteoclast activity by blocking autophagy caused by periodontitis, thereby reducing bone resorption. This study provides theoretical evidence for the role of YNBY in promoting osteogenic differentiation, specifically through the regulation of the autophagy pathway. Experimental evidence further supports the notion that excessive upregulation of autophagy in an inflammatory environment may inhibit osteogenic differentiation. The findings offer potential novel therapeutic strategies for periodontitis.

Ethics Approval and Informed Consent

All animal experiments in this study were approved by the Animal Experiment Ethics Review Committee of Kunming Medical University (Approval No. KMMU 20221850). The procedures applied adhered to the Chinese guidelines for the welfare of laboratory animals (GB/T 35823-2018) in all respects.

Acknowledgments

Author Contributions

All authors have contributed significantly to the work reported, whether in its conception, study design, execution, data acquisition, analysis and interpretation, or in all these areas. They participated in drafting, revising, or critically reviewing the article, provided final approval of the version to be published, agreed on the journal to which the article has been submitted, and consent to be accountable for all aspects of the work. All authors have thoroughly read and approved the final submitted manuscript.

Disclosure

The authors report no conflicts of interest in this work.

References

1. Armitage GC. Periodontal diagnoses and classification of periodontal diseases. *Periodontol*. 2004;34(1):9–21. doi:10.1046/j.0906-6713.2002.003421.x
2. Zhao J, Birjandi AA, Ahmed M, Redhead Y, Olea JV, Sharpe P. Telocytes regulate macrophages in periodontal disease. *Elife*. 2022;3:11.
3. Novello S, Tricot-Doleux S, Novella A, Pellen-Mussi P, Jeanne S. Influence of periodontal ligament stem cell-derived conditioned medium on osteoblasts. *Pharmaceutics*. 2022;14(4):729. doi:10.3390/pharmaceutics14040729
4. Cheat B, Torrens C, Foda A, et al. NLRP3 Is involved in neutrophil mobilization in experimental periodontitis. *Front Immunol*. 2022;13:839929. doi:10.3389/fimmu.2022.839929
5. Li N, Xie L, Wu Y, et al. Dexamethasone-loaded zeolitic imidazolate frameworks nanocomposite hydrogel with antibacterial and anti-inflammatory effects for periodontitis treatment. *Mater Today Bio*. 2022;16:100360. doi:10.1016/j.mtbio.2022.100360
6. Um S, Lee JH, Seo BM. TGF-beta2 downregulates osteogenesis under inflammatory conditions in dental follicle stem cells. *Int J Oral Sci*. 2018;10 (3):29. doi:10.1038/s41368-018-0028-8
7. Chang Y, Hsiao YM, Hu CC, et al. Synovial Fluid Interleukin-16 Contributes to Osteoclast Activation and Bone Loss through the JNK/NFATc1 Signaling Cascade in Patients with Periprosthetic Joint Infection. *Int J Mol Sci*. 2020;21:8.
8. Bu T, Ren Y, Yu S, et al. A low-phenylalanine-containing whey protein hydrolysate stimulates osteogenic activity through the activation of p38/ Runx2 signaling in osteoblast cells. *Nutrients*. 2022;14(15):3135. doi:10.3390/nu14153135
9. Boyce BF, Xing L. Functions of RANKL/RANK/OPG in bone modeling and remodeling. *Arch Biochem Biophys*. 2008;473(2):139–146. doi:10.1016/j.abb.2008.03.018

10. Lee HA, Park MH, Song Y, Na HS, Chung J. Role of Aggregatibacter actinomycetemcomitans-induced autophagy in inflammatory response. *J Periodontol*. 2020;91(12):1682–1693. doi:10.1002/JPER.19-0639

11. Nollet M, Santucci-Darmanin S, Breuil V, et al. Autophagy in osteoblasts is involved in mineralization and bone homeostasis. *Autophagy*. 2014;10 (11):1965–1977. doi:10.4161/auto.36182

12. Wang B, Khan S, Wang P, et al. A highly selective GSK-3beta Inhibitor CHIR99021 promotes osteogenesis by activating canonical and autophagy-mediated wnt signaling. *Front Endocrinol*. 2022;13:926622. doi:10.3389/fendo.2022.926622

13. Laha D, Deb M, Das H. KLF2 (kruppel-like factor 2 [lung]) regulates osteoclastogenesis by modulating autophagy. *Autophagy*. 2019;15 (12):2063–2075. doi:10.1080/15548627.2019.1596491

14. Onal M, Piemontese M, Xiong J, et al. Suppression of autophagy in osteocytes mimics skeletal aging. *J Biol Chem*. 2013;288(24):17432–17440. doi:10.1074/jbc.M112.444190

15. Piemontese M, Onal M, Xiong J, et al. Low bone mass and changes in the osteocyte network in mice lacking autophagy in the osteoblast lineage. *Sci Rep*. 2016;6(1):24262. doi:10.1038/srep24262

16. Fujiwara T, Ye S, Castro-Gomes T, et al. PLEKHM1/DEF8/RAB7 complex regulates lysosome positioning and bone homeostasis. *JCI Insight*. 2016;1(17):e86330. doi:10.1172/jci.insight.86330

17. Yao Q, Chang BT, Chen R, et al. Research advances in pharmacology, safety, and clinical applications of Yunnan baiyao, a traditional Chinese medicine formula. *Front Pharmacol*. 2021;12:773185. doi:10.3389/fphar.2021.773185

18. Liu J, Cai M, Yan H, et al. Yunnan Baiyao reduces hospital-acquired pressure ulcers via suppressing virulence gene expression and biofilm formation of Staphylococcus aureus. *Int J Med Sci*. 2019;16(8):1078–1088. doi:10.7150/ijms.33723

19. Ren X, Zhu Y, Xie L, Zhang M, Gao L, He H. Yunnan Baiyao diminishes lipopolysaccharide-induced inflammation in osteoclasts. *J Food Biochem*. 2020;44(6):e13182. doi:10.1111/jfbc.13182

20. Li Y, Liu W, Zhao R, et al. Yunnan Baiyao inhibits periodontitis by suppressing the autophagic flux. *Int Dent J*. 2023;1:3.

21. Wang Y, Xia C, Chen Y, Jiang T, Hu Y, Gao Y. Resveratrol synergistically promotes BMP9-induced osteogenic differentiation of mesenchymal stem cells. *Stem Cells Int*. 2022;2022:8124085. doi:10.1155/2022/8124085

22. Hao Y, Ren Z, Yu L, et al. p300 arrests intervertebral disc degeneration by regulating the FOXO3/Sirt1/Wnt/beta-catenin axis. *Aging Cell*. 2022;21 (8):e13677. doi:10.1111/acel.13677

23. Park SW, Kim J, Oh S, et al. PHF20 is crucial for epigenetic control of starvation-induced autophagy through enhancer activation. *Nucleic Acids Res*. 2022;50(14):7856–7872. doi:10.1093/nar/gkac584

24. Kuo CH, Zhang BH, Huang SE, et al. Xanthine derivative KMUP-1 attenuates experimental periodontitis by reducing osteoclast differentiation and inflammation. *Front Pharmacol*. 2022;13:821492. doi:10.3389/fphar.2022.821492

25. Vicencio E, Cordero EM, Cortes BI, et al. Aggregatibacter actinomycetemcomitans induces autophagy in human junctional epithelium keratinocytes. *Cells*. 2020;9(5):1221. doi:10.3390/cells9051221

26. Momen-Heravi F, Friedman RA, Albeshri S, et al. Cell type-specific decomposition of gingival tissue transcriptomes. *J Dent Res*. 2021;100 (5):549–556. doi:10.1177/0022034520979614

27. Ni K, Hua Y. Hydrogen sulfide exacerbated periodontal inflammation and induced autophagy in experimental periodontitis. *Int Immunopharmacol*. 2021;93:107399. doi:10.1016/j.intimp.2021.107399

28. Dang H, Chen W, Chen L, Huo X, Wang F. TPPU inhibits inflammation-induced excessive autophagy to restore the osteogenic differentiation potential of stem cells and improves alveolar ridge preservation. *Sci Rep*. 2023;13(1). doi:10.1038/s41598-023-28710-0

29. Gruber R. Osteoimmunology: inflammatory osteolysis and regeneration of the alveolar bone. *J Clin Periodontol*. 2019;46(Suppl 21):52–69. doi:10.1111/jcpe.13056

30. Hienz SA, Paliwal S, Ivanovski S. Mechanisms of Bone Resorption in Periodontitis. *J Immunol Res*. 2015;2015:615486. doi:10.1155/2015/615486

31. Ma Y, Qian Y, Chen Y, et al. Resveratrol modulates the inflammatory response in hPDLSCs via the NRF2/HO-1 and NF-kappaB pathways and promotes osteogenic differentiation. *J Periodontal Res*. 2023;3:1.

32. Tamura H, Maekawa T, Domon H, et al. Erythromycin restores osteoblast differentiation and osteogenesis suppressed by porphyromonas gingivalis lipopolysaccharide. *Pharmaceuticals*. 2023;16(2):303. doi:10.3390/ph16020303

33. Hirata N, Ichimaru R, Tominari T, et al. Beta-cryptoxanthin inhibits lipopolysaccharide-induced osteoclast differentiation and bone resorption via the suppression of inhibitor of NF-kappaB kinase activity. *Nutrients*. 2019;11(2):368. doi:10.3390/nu11020368

34. Mueller-Buehl AM, Tsai T, Hurst J, et al. Reduced retinal degeneration in an oxidative stress organ culture model through an iNOS-inhibitor. *Biology*. 2021;10(5):383. doi:10.3390/biology10050383

35. Baek I, Bello AB, Jeon J, et al. Therapeutic potential of epiphyseal growth plate cells for bone regeneration in an osteoporosis model. *J Tissue Eng*. 2022;13:20417314221116754. doi:10.1177/20417314221116754

36. Yasuda H, Shima N, Nakagawa N, et al. Osteoclast differentiation factor is a ligand for osteoprotegerin/osteoclastogenesis-inhibitory factor and is identical to TRANCE/RANKL. *Proc Natl Acad Sci U S A*. 1998;95(7):3597–3602. doi:10.1073/pnas.95.7.3597

37. Huang D, Zhao C, Li R, et al. Identification of a binding site on soluble RANKL that can be targeted to inhibit soluble RANK-RANKL interactions and treat osteoporosis. *Nat Commun*. 2022;13(1):5338.

38. Kadriu B, Gold PW, Luckenbaugh DA, et al. Acute ketamine administration corrects abnormal inflammatory bone markers in major depressive disorder. *Mol Psychiatry*. 2018;23(7):1626–1631. doi:10.1038/mp.2017.109

39. Uenaka M, Yamashita E, Kikuta J, et al. Osteoblast-derived vesicles induce a switch from bone-formation to bone-resorption in vivo. *Nat Commun*. 2022;13(1):1066. doi:10.1038/s41467-022-28673-2

40. Li Y, Su J, Sun W, Cai L, Deng Z. AMP-activated protein kinase stimulates osteoblast differentiation and mineralization through autophagy induction. *Int J Mol Med*. 2018;41(5):2535–2544. doi:10.3892/ijmm.2018.3498

41. Yao W, Dai W, Jiang JX, Lane NE. Glucocorticoids and osteocyte autophagy. *Bone*. 2013;54(2):279–284. doi:10.1016/j.bone.2013.01.034

42. Liu J, Wang Y, Shi Q, et al. Mitochondrial DNA efflux maintained in gingival fibroblasts of patients with periodontitis through ROS/mPTP pathway. *Oxid Med Cell Longev*. 2022;2022:1000213. doi:10.1155/2022/1000213

43. Kang Y, Kong N, Ou M, et al. A novel cascaded energy conversion system inducing efficient and precise cancer therapy. *Bioact Mater*. 2023;20:663–676. doi:10.1016/j.bioactmat.2022.07.007

44. Liu C, Mo L, Niu Y, Li X, Zhou X, Xu X. The role of reactive oxygen species and autophagy in periodontitis and their potential linkage. *Front Physiol.* 2017;8:439. doi:10.3389/fphys.2017.00439

45. Greabu M, Giampieri F, Imre MM, et al. Autophagy, one of the main steps in periodontitis pathogenesis and evolution. *Molecules.* 2020;25 (18):4338. doi:10.3390/molecules25184338

Journal of Inflammation Research

Dovepress

Publish your work in this journal

The Journal of Inflammation Research is an international, peer-reviewed open-access journal that welcomes laboratory and clinical findings on the molecular basis, cell biology and pharmacology of inflammation including original research, reviews, symposium reports, hypothesis formation and commentaries on: acute/chronic inflammation; mediators of inflammation; cellular processes; molecular mechanisms; pharmacology and novel anti-inflammatory drugs; clinical conditions involving inflammation. The manuscript management system is completely online and includes a very quick and fair peer-review system. Visit http://www.dovepress.com/testimonials.php to read real quotes from published authors.

Submit your manuscript here: https://www.dovepress.com/journal-of-inflammation-research-journal

---